SZENT ISTVÁN UNIVERSITY

# Performance enhancement of solar air collectors applied for drying processes

Thesis of PhD work

by

Maytham Ali Jasim Al-Neama

Gödöllő
2018

**Doctoral school**

**Denomination:** Mechanical Engineering PhD School

**Science**: Solar Energy Applications

**Leader:** Prof. Dr. István Farkas
Dr. of Technical Sciences
Faculty of Mechanical Engineering
Szent István University, Gödöllő, Hungary

**Supervisor:** Prof. Dr. Farkas István
Dr. of Technical Sciences
Faculty of Mechanical Engineering
Szent István University, Gödöllő, Hungary

…… ……

Affirmation of supervisor Affirmation of head of school

CONTENTS

# 1. INTRODUCTION, OBJECTIVES

Solar drying is one among the common applications of solar energy utilization. Solar drying is one of the oldest methods of preservation of agricultural products and it is utilized everywhere. Solar drying is a dual process of heat transfer to the product items from the heat source (solar collector) and mass transfer in the form of moisture content from the product to product's surface and then to the surrounding air. Solar drying systems are available in the different design and sizes according to dried products capacity.

According to many studies, the performance of drying process depends mainly on the performance of solar collector. The improvement of solar air collector improvement produce enhancement in the dryer work also. But, some products do not need for high air temperature because it will damage such as fish, meats, etc. So, the control of the process parameters, air temperature, moister content for air and product and airspeed critical.

In the present research, comprehensive evaluation of different designs of solar collector integrated with drying chamber will be performed according to heat transfer basses to enhance the thermal performance of the total system. Additionally, to show the effect of each parameter on system behaviour under Gödöllő city climatic conditions. Based on the results achieved so far in the studied previous works, during the forming of the aims of the recent PhD work, it was a strong initiation for an experimental improvement for the solar air collectors carried out to enhance the process of drying. The shape and dimensions of absorbing surfaces are tested. The objectives of this research can be described as follow:

- Comparison of single-pass solar air collector thermal performance for drying process with the double-pass solar air collector performance experimentally.
- Investigation of solar air collector thermal behaviour experimentally by using five shapes of absorbers: un-finned absorber, absorber with horizontal rectangular fines, absorber with vertical rectangular fines, absorber with $45^{o}$ inclined rectangular fines and absorber with aluminium helical fines.
- Test the performance of drying chamber experimentally by integrating it with five shapes of absorbers: un-finned absorber, absorber with horizontal rectangular fines, absorber with vertical rectangular fines, absorber with $45^{o}$ rectangular fines and absorber with aluminium helical fines.
- Estimation of thermal daily efficiency of the tested solar air collectors.
- Investigation the effect of air movement method and air velocity on the thermal daily efficiency of solar air collector with forced and natural mode by using a circular chimney.
- Estimation the weight loss of dried product items by using different tested types of solar air collectors.

## 2. MATERIALS AND METHODS

In this chapter, the used materials and methods for experimental investigation and theoretical analysis are discussed concerning to the solar test rig consists of many principal components to achieve study objectives. Solar drying system consists mainly of solar air collector, drying chamber, chimney, photovoltaic module and inline air blower.

### 2.1. Solar collectors location and orientation

The location of the solar collectors is a critical aspect of efficient sun energy collection. The factor of shadowing should be considered (trees or surrounded buildings). Collector's location has been chosen according to the fact that the shadow effect will have no impact on the collector efficiency. The orientation of the solar collector is described by its azimuth and tilt angles. The optimum tilt angle (β) and direction play an important factor in enhancing solar energy collection of solar collectors. Flat plate solar collector, it is always tilted in such a way that it receives maximum solar radiation during the day and to be perpendicular to solar radiation rays at noon.

The best stationary orientation is due south in the northern hemisphere and due north in the southern hemisphere. Therefore, the solar air collectors in this work are oriented facing south line and tilted at 45$^{o}$ to the horizontal according to the solar chart for the region as shown in Fig. 1 (47.59$^{o}$ N, 19.36$^{o}$ E).

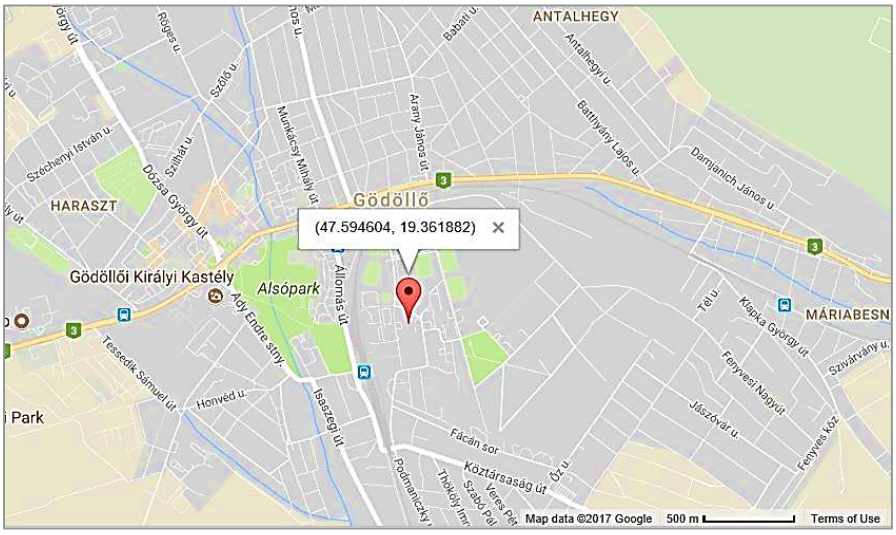


Fig. 1. Latitude and longitude of experiments location

### 2.2. Design and structure of solar collectors

The flat plate solar air heater has the same method of the heat exchanger, convert solar radiation energy into heat energy, which is passed on through convection from the absorber plate to the air. In the present work, three solar air collectors are designed and built in mechanical engineering department laboratory in Szent Istvan University. The first solar collector is single air pass while second and third are double air pass solar collectors. The main parts of each; absorbing surface, external box, transparent glass cover, and back insulation. These parts are explained in details in the next sections.

For study purpose, five absorbing surfaces are made from copper plate sheet with 1.2 mm thickness and thermal conductivity 385 W/m K as shown in Fig. 2. To enhance these surfaces (selective

surface) a black matt paint (black chrome) used to coat copper absorbing surfaces. Selective surfaces combine a high absorptance for radiation with a low emittance for the temperature range in which the surface emits radiation. Black paint also enables much of the absorbed energy to be lost by emittance.

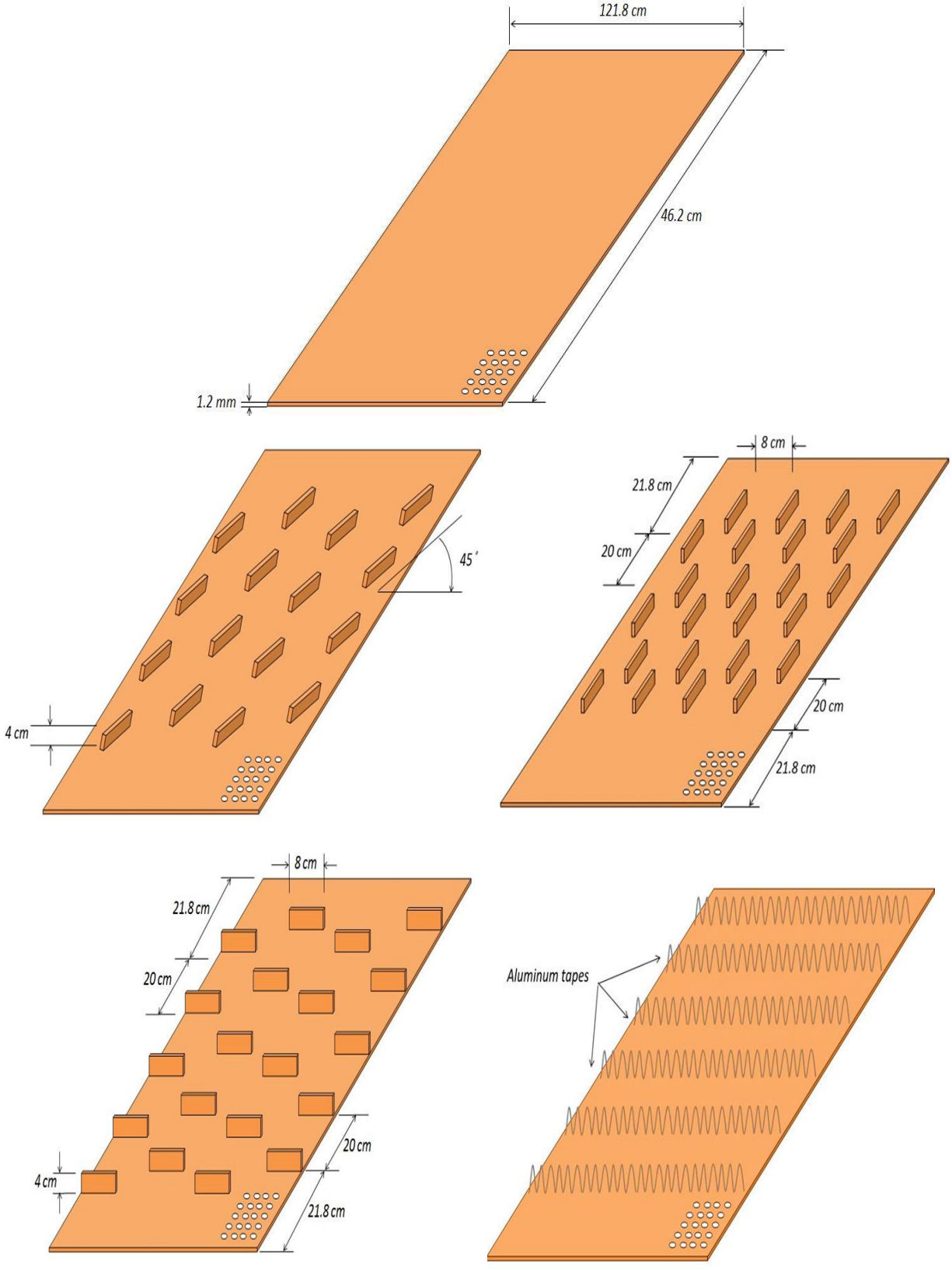


Fig. 2. Different shapes used absorbing surfaces dimensions

The first is flat absorber (un-finned) with dimensions 46.2×121.8 cm length and width respectively. The second and third absorbing surfaces had made with the same dimensions of the the first surface with horizontal and vertical 18 fins to increase its area of surface. The forth is made with 45$^{o}$ rectangular fins. An aluminium helical fins are attached to the copper surface of the fifth absorbing surface. Fins function is expanding air stream length with the absorber surface to improve the useful heat transfer to the air. The space between every two lines of fins was 17 m. for double pass collector, 25 holes made on the absorber with the same area of the air inlet and exit to recirculate the air from the first to the second air channel. The dimensions of rectangular fin are 4 cm and 10 cm length and width respectively. The helical fins had been made from aluminium sheets with thickness 0.5 mm and fixed on the absorbing surface. The dimensions of fin are 66.2 cm and 4 cm length and width respectively. Nine fins are attached on absorbing and painted by black matt paint.

The external dimensions of solar heater are 120×50×15 cm length, width and thickness respectively. The external box of solar collectors is made from wood sheets and bars with different thicknesses with dimensions. Wood had been chosen for many important reasons that were taken into account which are lighter in weight rather than using metal, the low cost, easy to form and can be considered as insolation specially at very low temperatures. The second air channel of double pass solar collector was designed with many attached buffers which fixed on back surface of solar collector. Buffers function is to increase air stream length with the absorber surface to enhance the useful heat transfer to the air.

The space between every two buffers is 17 m. Wooden-made zigzag baffles are attached in the lower channel in order to give homogenous air distribution under absorber surface. The areas of inlet, exit and second channel entrance of solar air collector are the same, to avoid pressure reduction through solar air collector. The sides of the body were well insulated to prevent heat loss by using self-adhesive rubber foam tape with thickness of 3 mm. Fig. 3 show the first and second channels of solar air collector with details.

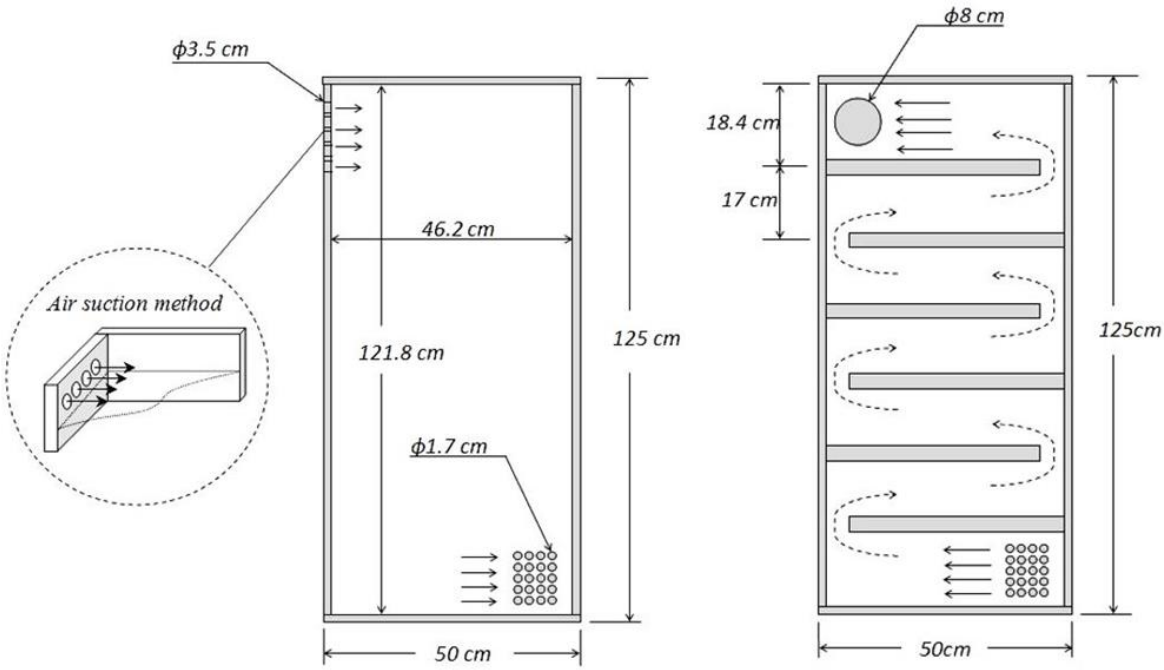


Fig. 3. First and second air pass of solar air heaters design

At the back side of the collector, sheets of expanded polystyrene insulation (EPS) with smooth edges fixed at the bottom base side of the wooden box. The heat transfer coefficient of back insulation is 0.036 W/mK. Back insulation thickness is 2 cm and dimensions are 120×50 cm length and width respectively. The sides of the body were well insulated to prevent heat loss by using self-adhesive rubber foam tape with thickness of 3 mm.

A transparent glass cover fixed on the top edges of the heater wood case and thermal insulation at the bottom base side of the wooden case. The transparent cover made from high quality hard thermal plastic glass with 4 mm and 0.16 W/mK thickness and heat transfer coefficient, respectively. Cover dimensions are 120 cm×50 cm length and width respectively. The remaining space between the absorber plate and glass cover represents the upper air flow channel with 57.5 mm height. It is important in the solar air collector components arrangements, tight any air leakage because the leakage of air will effect on the performance of the solar collector (especially air temperature) and decrease its thermal efficiency.

### 2.3. Design and structure of drying chambers

The second essential part of drying system is drying chamber (drying cabin). In this study, polystyrene blocks with 5 cm thickness and thermal conductivity 73 W/m K had been used to build drying chamber. This material was used due to many important reasons; which are low thermal conductivity (insulated), cheap, easy to preform it and light. The drying chamber (the dryer) with five trays for the different products items is made from. The drying cabin dimensions are 50 cm×50 cm×100 cm length, width, and height, respectively as shown in Fig. 4. Dryer walls have been made from polystyrene, except the front wall of the chamber made from 4 mm plastic glass sheet for observing. The five trays made from plastic nets and fixed with 10 cm distance between them as shown in Fig. 5. The dimensions of every tray are 38 cm×40 cm length and width respectively.

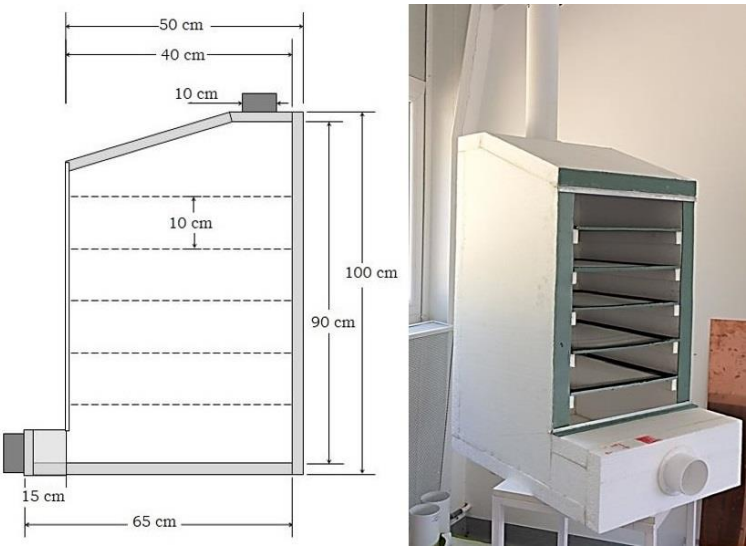


Fig. 4. Drying chamber dimensions and illustration

The chamber is integrated with the solar collector by a small duct (indirect drying), then the exit heated air from the collector enters the chamber with high temperature and low humidity. The moist and hot air rises and escapes from the upper vent of drying chamber. Inlet and outlet of drying chamber have a diameter 10 cm with a small slop angle for the upper side of the chamber to keep the smooth movement of the air.

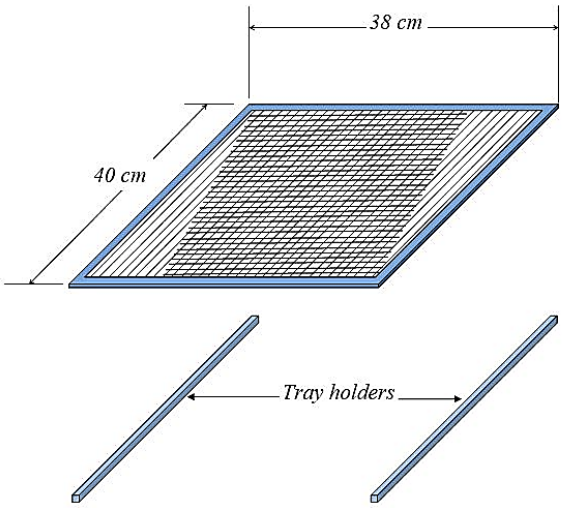


Fig. 5. Tray dimensions and installation

Also, all air leakages from drying space closed totally as possible. The product sample which used through this study is apple. Apple selected as a sample because of its high initial moisture content and its high maximum allowable temperature. The initial moisture content and maximum allowable temperature for apple during drying process are 80% (wet base) and 70 $^{o}$C respectively.

### 2.4. Solar drying system accessories

Many accessories and minor devices are arranged with the solar drying system to achieve the purpose of this experimental work such as air blower, photovoltaic module, electrical power supply regulator, and insulated air ducts.

To circulate the air through the solar drying system, air inline blower in air duct between solar heater and drying chamber has been used. The suction and discharge of blower is bigger than ducts with 10.5 cm diameter. The blower works with 12 V and 270 CFM. A circulation duct of 10 cm diameter is used to circulate air through the solar drying system. These ducts were insulated by using a 1 cm thickness of special type of polystyrene to decrease heat loss to the surroundings.

A two photovoltaic modules were installed in the same direction and tilt angle of solar air collectors to supply the electrical power to the blowers. The modules are connected to power supply regulator to supply constant voltage. The modules system voltage is 12 V. A laboratory power supply controller type Voltcraft PS 1440 was using to supply and control the electrical power to the solar air collector blower and to regulate the outlet voltage therefore the velocity can be changed indeed. The working ranges for this device are 0-36 V/DC, 0.01-40 A voltage and current respectively.

An insulated air ducts have been connected the essential components of solar drying system. The ducts are insulated with a 10 mm special type of polystyrene to decrease heat loss to the surroundings and fixed carefully. The diameter of air ducts is 10 cm with different lengths which depend on the positions of solar units.

### 2.5. Installation and measurements

The constructed solar air collectors and drying chamber were fixed at the laboratory and mounted to the south on an iron simple frame as shown in Fig. 6. The schematic diagram of the entire solar

drying system is illustrated in Fig. 7. The system designed, manufactured and installed in the open laboratory area of department of physics and process control, Szent István University. Insulated air ducts have connected the main components. Temperature, humidity, solar radiation, and airspeed were measured.


Fig. 6. Solar drying system illustration in laboratory

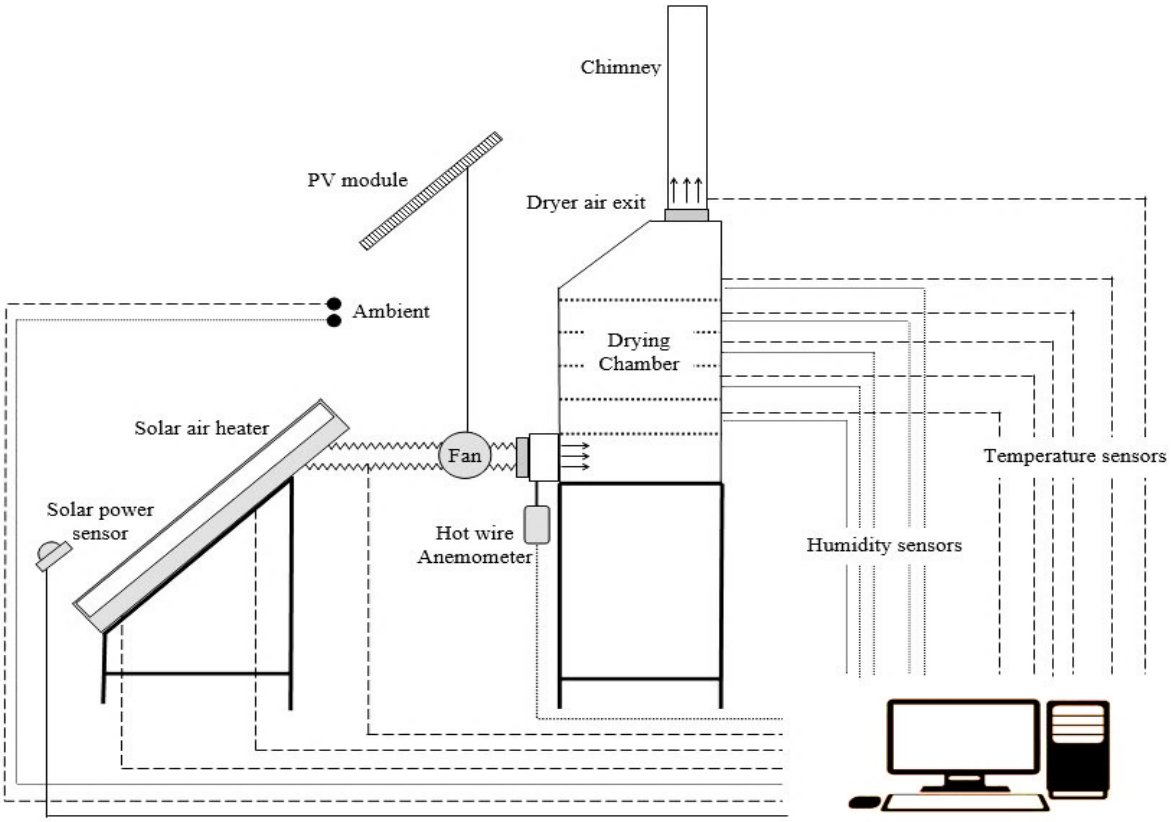


Fig. 7. Schematic diagram of solar drying system

Many sensors have been fixed in many points of the system to measure system variables, then logged them on the computer to analysis them for system performance investigation. The blowers are connected to the power supply which connected to the photovoltaic modules.

The following characteristics were measured to get the experimental results then analysing them to calculate the efficiency and the performance parameters of solar drying system as:

- The temperature measurements.
- Air speed measurements.
- Global solar radiation intensity measurement.
- Air relative humidity measurements.
- Initial and final weight of dried product items.

The temperatures in different points of solar air heater needs to be measured to achieve the temperature distribution. For this purpose, the K-type twisted thermocouples wire were used as shown in Fig. 8.

The global solar radiation is measured by a digital solar power meter with its sensor. It is placed on the same tilt angle of the collector at the same direction. The spectral response of solar meter from 400 to 1100 nm and measurement range varies from 1 W/m$^2$ to 1300 W/m$^2$.

A MS6252A digital anemometer instrument was used to measure the air velocity then the air mass flow can be calculated by multiplying with the cross-section area and the air outlet density as shown in Fig. 8. The measuring range is 0.4-30 m/s. The anemometer woks with power supply 9 V. The accuracy is ±2% with mentioned working range. The air flow rate had been measured in the inlet and outlet of solar system with a constant voltage power supply to air blower.

Five points on the trays of drying chamber and one point for ambient. A digital humidity meters with their sensors are used. The measuring range for these meters varies from 10% RH to 99% RH with humidity accuracy ±4%. Humidity meter display resolution is 1% RH and measuring temperature range from -50 °C to +70 °C. It has dimensions 4.8×2.8×1.5cm and working with 2×1.5 V batteries. Sensor cable length is 1.5 m with probe length 6 cm.


Fig. 8. Experimental measurements instruments

# 3. RESULTS

The present chapter displays the most important achieved results and their discussion.

## 3.1. Effect of air passes number

*Single air pass solar collector experimental analysis*

The experimental data of single-pass solar collector have been recorded with 10min constant time step from 10:00 to 15:00 of 2nd of October 2017. The collector arranged to drying chamber with dried items (apple slices) by inline air blower with 2.3 m/s air velocity.

Fig. 9 showed the solar radiation intensity variation and calculated useful heat during 5 hours of experiments days. The maximum radiation intensity was 948 W/m$^2$ at noon. The solar radiation blocked by some sporadic clouds between 12:40 and 13:40. The useful heat obtained from the solar air collector was proportional directly to the values of temperature change through the solar collector. The useful heat increases to reach the maximum value 230 W/m$^2$ at the same time of maximum temperature differences at 11:30.

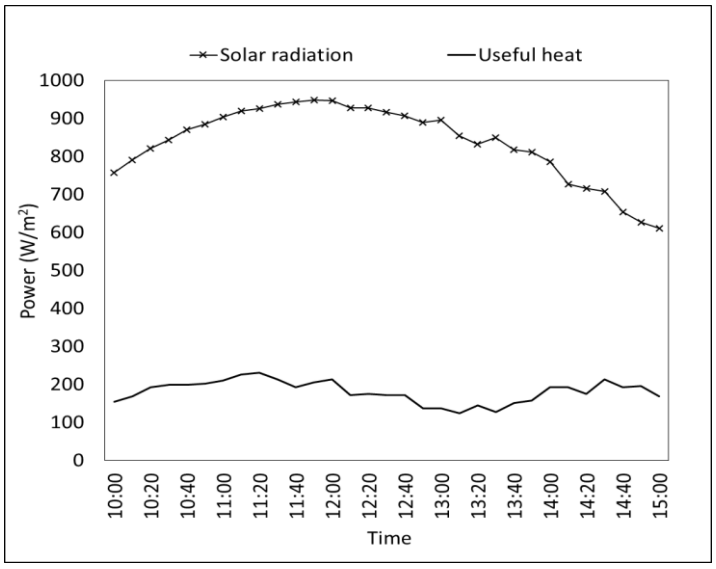


Fig. 9. Useful gained heat and solar radiation intensity vs time

The performance of single-pass solar air collector can be represented in the form of relation between thermal efficiency of solar air collector and (($T_{s,av}$ - $T_a$ )/ I) according to the slandered test of solar collectors. The closest obtained curve in Fig. 10 shows a linear relationship between the horizontal and vertical axes, where *x* represents the term of (($T_{s,av}$-$T_a$)/ I), while *y* represents the thermal efficiency of solar collector (η, %). So, the linear model formula as following:

$$\eta = a \frac{T_{av,s} - T_a}{I} + b. \quad (1)$$

The parameters of linear equation $a$ and $b$ can be obtained mathematically for the range of experimental cases for single-pass solar collectors group:

$$a = -3308.3 \ and \ b = 168.8.$$

During the approximation the correlation coefficient was 0.42 along with the standard deviation of 7.76%. The model represents the closest expression of the relationship between temperature

difference, solar radiation intensity and thermal instantaneous efficiency. The developed theoretical model can be applied in the range of 0.036 and 0.0415 of $((T_{s,av} - T_a)/ I)$.

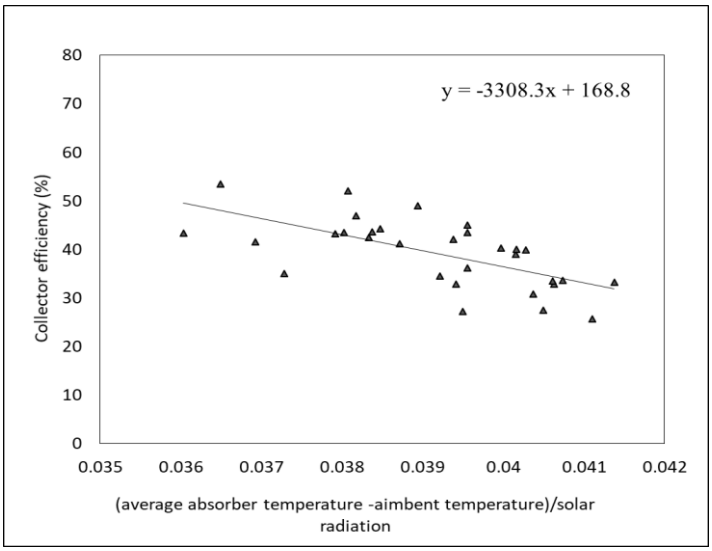


Fig. 10. Performance diagram of single-pass solar air collector

*Double air pass solar collector experimental analysis*

The experimental results have been recorded under same working conditions of single air pass solar collector with 10min constant time step from 10:00 to 15:00 of 2nd of October 2017. The double solar collector with a flat absorbing surface had been arranged to drying chamber which contains the apple slices (dried items) by a small inline air blower with 2.3 m/s air velocity.

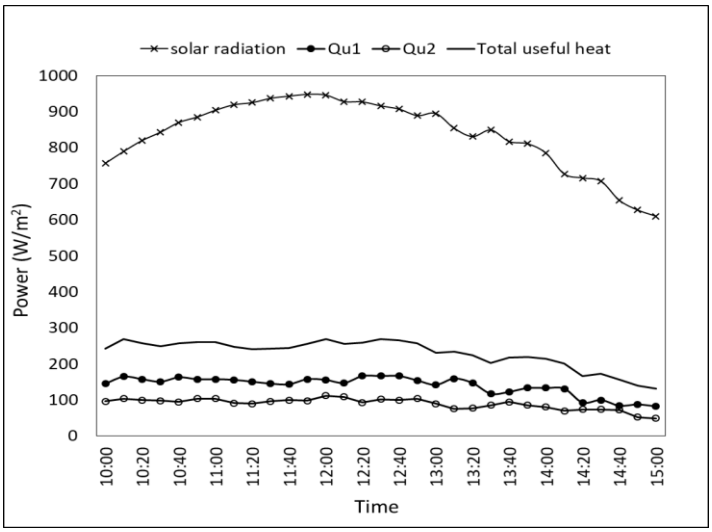


Fig. 11. Useful gained heat and solar radiation intensity vs time

The measured solar radiation intensity irradiance curve and calculated total useful heat during 5 hours of experiments days are shown in Fig. 11. The maximum radiation intensity was 948 W/m$^2$ at noon. The solar radiation blocked by some sporadic clouds between 12:40 and 13:40. The useful heat consists of two components; first is upper channel useful gained heat and the second is the lower channel useful gained heat. The figure obtained that the useful heat gained curves were proportional directly to the solar radiation intensity and air temperature difference through the collector. The two channels useful heat increases to reach the maximum values 166.5 and 112.2

$W/m^2$ at the same time of maximum temperature differences. The total useful heat of solar collector is the summation of two channels useful heat. The values of upper pass useful heat are higher than lower channel due to the high-temperature difference in the upper channel and direct sun heated.

By the same way of single-pass solar collector, the performance of double-pass solar air collector has been investigated according to the standard test of solar air collectors as shown in Fig. 12. The obtained relationship can be represented by a linear model in Eq. (1). The parameters of *a* and *b* can be obtained mathematically for the range of experimental cases for double-pass solar collectors group:

$$a = -1881.8 \ \ and \ \ b = 63.09.$$

During the approximation the correlation coefficient was 0.335 along with the standard deviation of 3.62%. The theoretical model can be applied in range of 0.0078 and 0.0123 of $((T_{s,av} - T_a)/ I)$. The values of constants are much less than the obtained with using single-pass solar collector, because the values of *x* axis of double-pass are less than single-pass values. The slope of performance line by single-pass solar collector higher than double-pass solar collector.

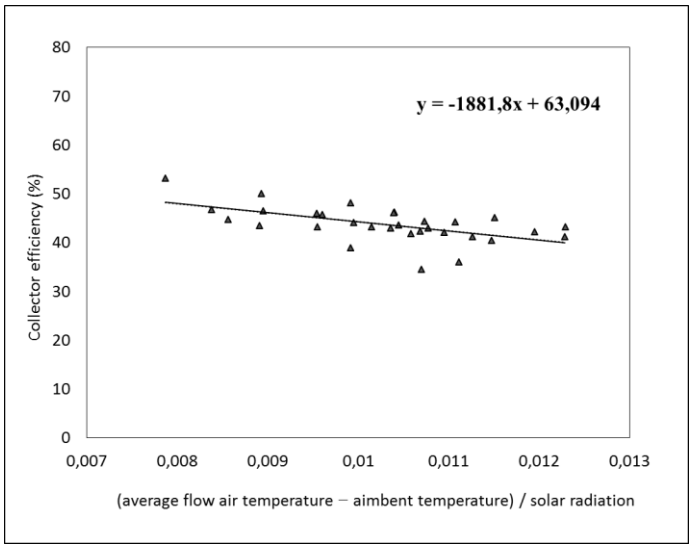


Fig. 12. Performance diagram of double-pass solar air collector

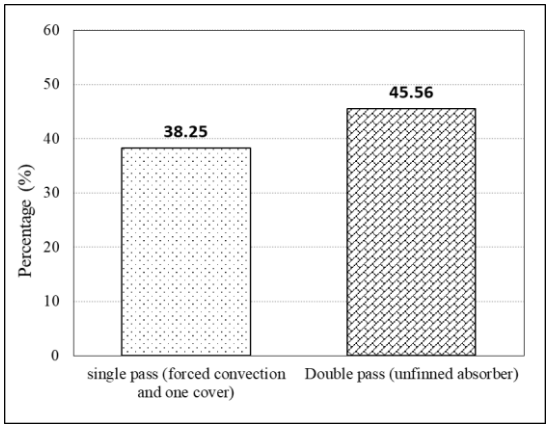


Fig. 13. Daily efficiency of single and double-pass solar air collectors

Fig. 13. shows the improvement of flat plate solar air collector's efficiency by increasing number of air passes. The calculated daily efficiency of the single-pass solar collector is 38.25%, while it

is 45.56% for double-pass solar air collector. Actually, the main reason for that increase is the increasing of heat transfer area between the absorbing surface and flowed air. In this study, the value of efficiency improvement by duplicating air pass was very agreed with the past works with the acceptable difference due to the different location and weather conditions of the experiments.

### 3.2. Effect of direction and shape of extended surfaces

The experimental data of horizontally finned plate double-pass solar air collector have been collected with 10min constant time step from 10:00 to 15:00 of 12 of October 2017.

The instantaneous useful heat for two channels of horizontally finned plate double pass solar air collector and solar radiation intensity is plotted with the time in Fig. 14. The curve of solar radiation has some fluctuated points due to some clouds. The values of gained heat are higher than the rates which recorded with using flat plate solar collector in the previous section. The maximum value of total useful heat was 408.1 W/m$^2$ at 12:30.

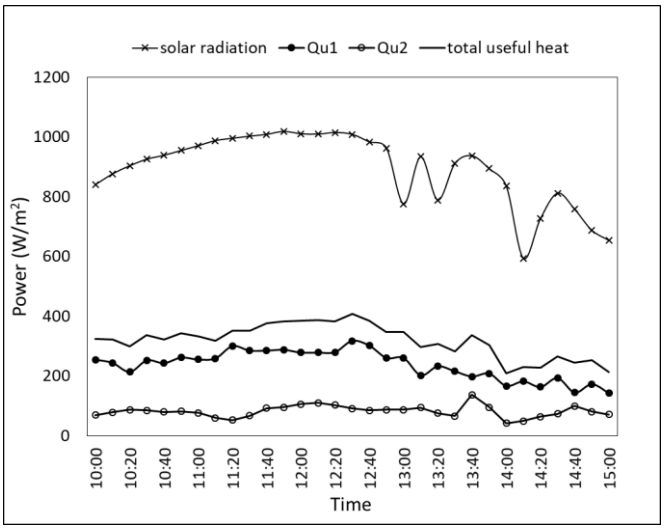


Fig. 14. Useful heat of horizontally finned plate solar collector and radiation intensity vs time

In the second set, the fins are inclined 45$^o$ to show the effect of fins direction on the thermal performance of solar air collector and drying chamber. The experimental data of 45$^o$ finned plate double-pass solar air collector have been collected with 10min constant time step from 10:00 to 15:00 of 9 of October 2017.

Fig. 15 shows the plotted instantaneous useful heat for the two channels of 45$^o$ finned plate double-pass solar collector and solar radiation intensity with the time. As shown, the curve of solar radiation intensity has very stable rates during the day. The maximum recorded solar radiation is 1066 W/m$^2$ at 12:00. The values of gained heat are lower than the rates which recorded by using horizontally finned plate collector in the previous section.

The highest useful heat is 355.5 W/m$^2$ at 12:30 because of the highest levels of solar radiation intensity and solar collector temperature difference. The extended surfaces attachment are not increasing heat transfer area only; it is increasing the turbulence of flowed air through solar collector which increase surface temperature.

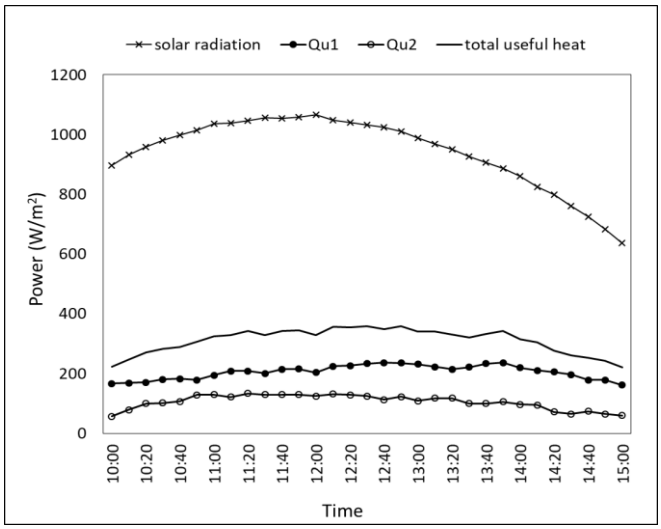


Fig. 15. Useful heat of 45° inclined finned plate double-pass collector and solar radiation intensity vs time

In the third set of experimental results, the rectangular vertical fins (parallel to air stream flow) are integrated with absorbing surface. The experimental data of vertically finned plate double-pass solar air collector have been graphed and reported with 10min constant time step for five hours from 10:00 to 15:00 of 12 of October 2017.

Fig. 16. shows the instantaneous useful heat variation for the upper and lower channels of vertically finned plate double-pass solar collector and solar radiation intensity with the time. As shown, the curve of solar radiation intensity has very fluctuated rates after 12:40. The maximum recorded solar radiation is 1017 W/m$^2$ at 12:00. The values of gained useful heat are lower than the values which recorded by using horizontally and 45° finned plate solar collector in the previous sections. The highest useful heat is 328 W/m$^2$ at 11:50 because of the highest levels of solar radiation and solar collector temperature differences.

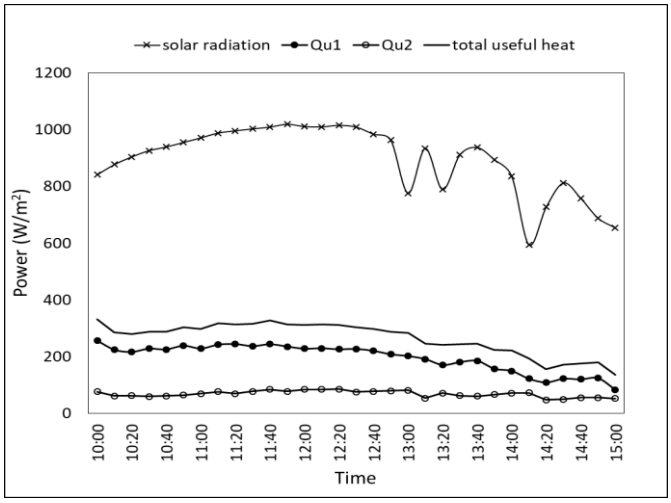


Fig. 16. Useful heat of vertically finned plate solar collector and solar radiation intensity vs time

The effect of fins direction with the thermal efficiency of double-pass solar air collector is obtained in Fig. 17. The horizontal (0°) showed the highest efficiency compared with the other angles. The experimental curve shows an inverse relation between fins angle and thermal efficiency.

Theoretically, a second order polynomial model gives the closest shape for relation, where *x* axis

represents the angle of rectangular fins $\psi$, while *y* axis represents the thermal efficiency of solar collector ($\eta$) as following:

$$\eta = a\,\psi^2 + b\,\psi + c. \quad (2)$$

The parameters *a*, *b* and *c* of polynomial model are calculated analytically for the case of rectangular finned double-pass solar air collectors groups, as follows:

$$a = -0.0006,\ b = -0.0536\ and\ \ c = 55.975.$$

During the approximation the correlation coefficient was 0.99 along with the standard deviation of 3.9%. The first term can be neglected if the angle is very small due to low value of *a* parameter. The efficiency is a function of the geometry of surface.

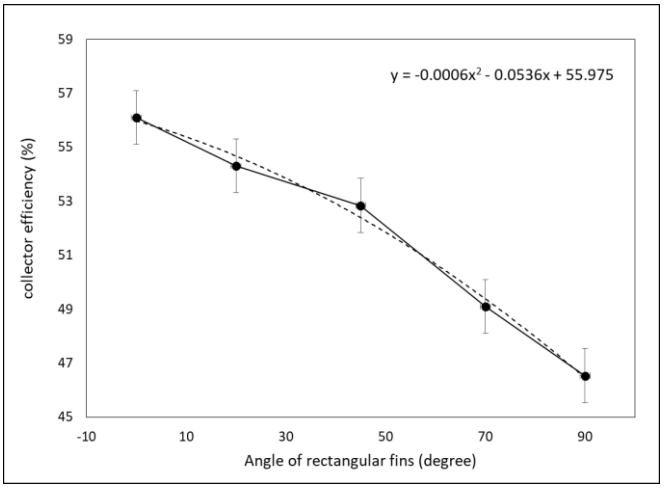


Fig. 17. Relationship between rectangular fins direction and collector thermal efficiency

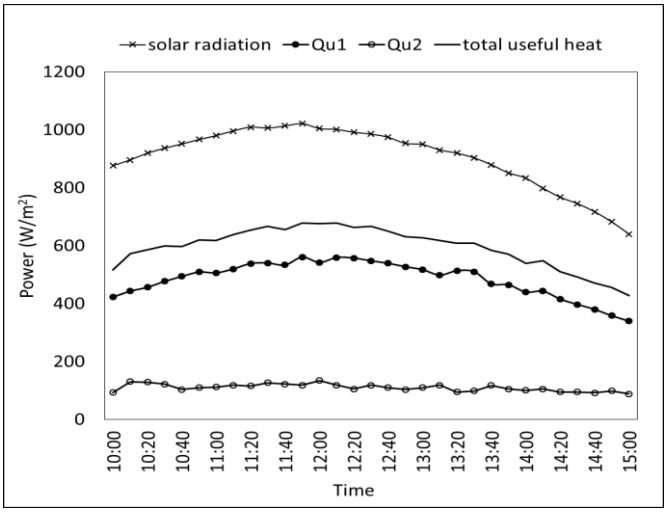


Fig. 18. Useful heat of helically-finned plate solar collector and solar radiation intensity vs time

In the last set, the aluminium helical fins are integrated with absorbing surface. The experimental data of helically-finned plate double-pass solar air collector have been collected with 10 min constant time step for five hours from 10:00 to 15:00 of 26 April 2018. The conditions of climate were very clear with some part small clouds. Fig. 18 explains the plotted instantaneous useful heat gained for the two channels of helically-finned plate double-pass solar collector and solar radiation intensity with the time. The maximum recorded solar radiation is 1021 W/m$^2$ at 12:00. The values of useful gained heat are higher than the rates which recorded by using un-finned, horizontally

finned, vertically finned and 45° finned plate solar air collectors in the previous section. The highest useful gained heat is 678.6 W/m$^2$ at 12:00 because of the highest levels of solar radiation intensities and solar collector temperature differences.

Fig. 19. shows the improvement of double-pass solar air collector's efficiency by change absorbing surface's area and shape. The daily efficiency is calculated for five types of absorbing surfaces solar collectors; flat plate, horizontally finned plate, 45° finned plate, vertically finned plate and helically-finned plate solar collectors. As shown, the thermal efficiency of double-pass solar air collector hadn't significant improvement with about 1% by integrating vertical rectangular extended surfaces (fins). This is because two main reasons, first is the direction of fins parallel to the direction of air flow and the second is the extended surfaces are not exposed in an optimum way to the solar radiation.

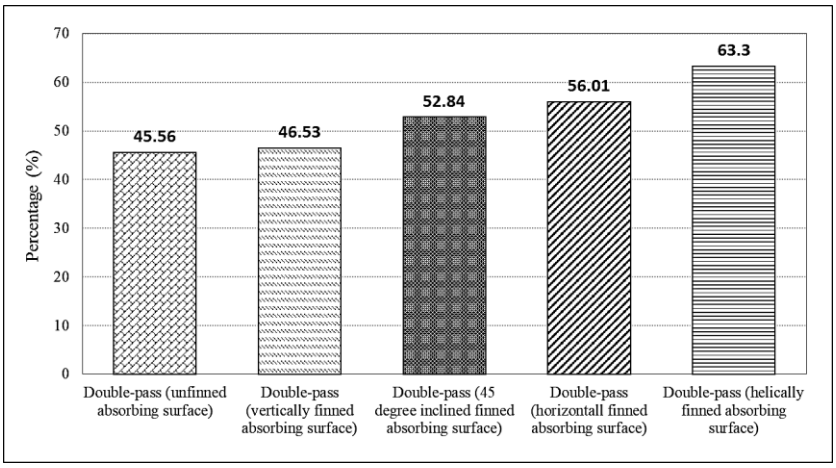


Fig. 19. The daily efficiency of finned and un-finned double-pass solar air collectors

### 3.3. Effect of air mass flow rate

*Forced air movement*

In order to estimate the effect of air flow rate, the flat plate double-pass solar air collector examined experimentally with different values of air mass flow rates.

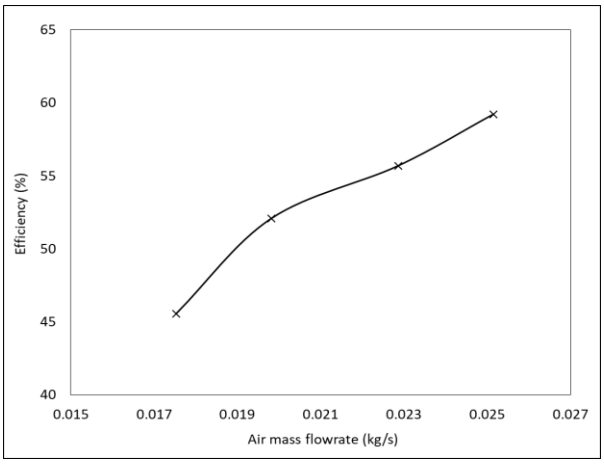


Fig. 20. The relation between air mass flow rate variations with the daily efficiency of collector

As shown in Fig. 20, the mass flow rate of air has a sufficient effect on the thermal efficiency of solar air collector. As shown, the thermal efficiency of double-pass solar air collector varies

indirectly with air mass flow rate variation. The solar air collector investigated with four values of air mass flow rate 0.0175, 0.0198, 0.0228 and 0.025 kg/s. The highest value of thermal efficiency was about 59% at 0.0251 kg/s air mass flow rate, while the lowest values was approximately 45.5% at 0.0175 kg/s.

*Natural air movement by chimney effect*

The integrated chimney has a circular cross-section and 1.5 m length. The experimental results are collected in 9 of October 2017 with free air velocity. Fig. 21 explains the variation of air speed with solar radiation intensity variation for two radiation ranges.. The speeds increased sharply at the beginning of experiment due to temperature increase. A second order polynomial model is the closest expression which represent the behaviour, where *x* represents the intensity of solar radiation *I*, while *y* represents the speed of air through chimney $V_{ch}$ as following:

$$V_{ch} = a\, I^2 + b\, I + c. \tag{3}$$

To find the final model, the numerical constants *a*, *b* and *c* of polynomial model are calculated analytically for solar radiation range from 600 W/m$^2$ to 1100 W/m$^2$ as follows:

$$a = 10^{-6},\ b = -0.002\ and\ \ c = 1.3806.$$

The correlation coefficient was 0.96 along with the standard deviation of 0.075 m/s.

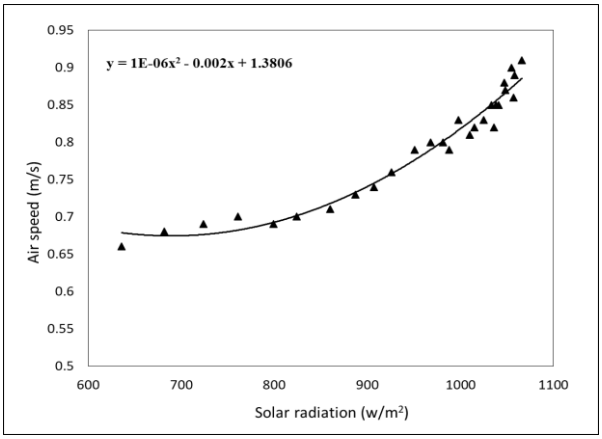


Fig. 21. The chimney air speed of drying system with solar radiation intensity variation

Fig. 22 shows the variation of chimney air speed with the absorber plate temperature. The increasing of absorber temperature leads to the more useful heat gained to the air. The temperature rise of air decrease the density of air which results a bouncy force. The design of solar chimney plays important rule to increase the speed of air due to the angle of entrance and length. The little slope which done in the top of drying chamber leads to smooth movement of air flow.

A linear model has been obtained to state the relation between air speed in chimney and average absorbing temperature as following:

$$V_{ch} = a\, T_{s,av} + b. \tag{4}$$

As mentioned before, the numerical constants are estimated analytically for absorber temperature range between 70 and 83 $^{o}$C with the following values:

$$a = 0.016 \quad a\ and\ d\ \ b = -0.4709.$$

The correlation coefficient was 0.57 along with the standard deviation of 0.082 m/s.

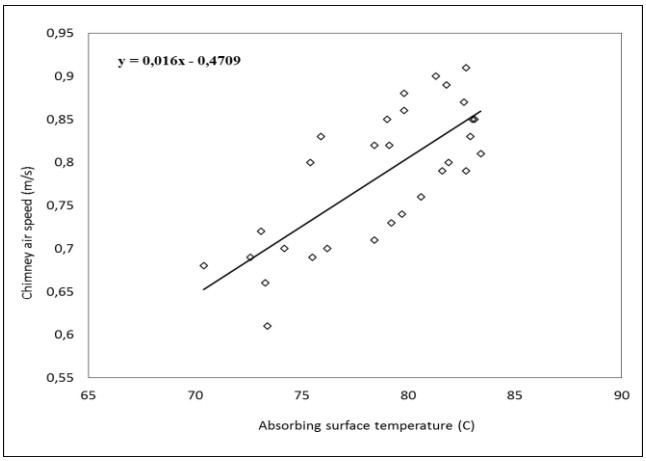


Fig. 22. The chimney air speed of drying system with absorbing surface temperature variation

### 3.4. Final weight analysis of dried product

The total final weight of dried product by using different types of solar collectors is shown in Fig. 23. Apple selected as a sample because of its high initial moisture content and its high maximum allowable temperature. The initial moisture content and allowable temperature for an apple during drying process are 80% (wet base) and 70 $^{o}$C respectively. The total initial weight of the dried product is 2000 g which scaled by a laboratorian weight scale and average initial moisture content 80%. The average diameter of slices is 65mm with 4 mm as an average thickness. The product (apple) are cut into approximately equal thicknesses slices and divided into five sets with 400 g.

The best result was with using a helically-finned plate double-pass solar air collector with final weight 937 g (lost about 53% of its initial weight). The using of double-pass solar air collector enhanced water content missing from 28% to 38% compared d with single-pass solar air collector. The attaching of horizontal fins to the double-pass solar collector enhanced the process from 38% to 42% compared with flat plate double-pass solar collector. The changing of fins direction affected on the final weight of the dried product. As shown, the vertical and 45$^{o}$ finned plate solar collectors were less efficient than horizontal finned solar collector as well the thermal efficiencies which mentioned in the previous sections. The final moisture contents for apple slices were approximately between 40 and 50% for the different types of tested solar air collectors. The final moisture content showed a good agreement for the short time of drying process (5 hours) and compared with 24% as a desired final moisture contents for apple.

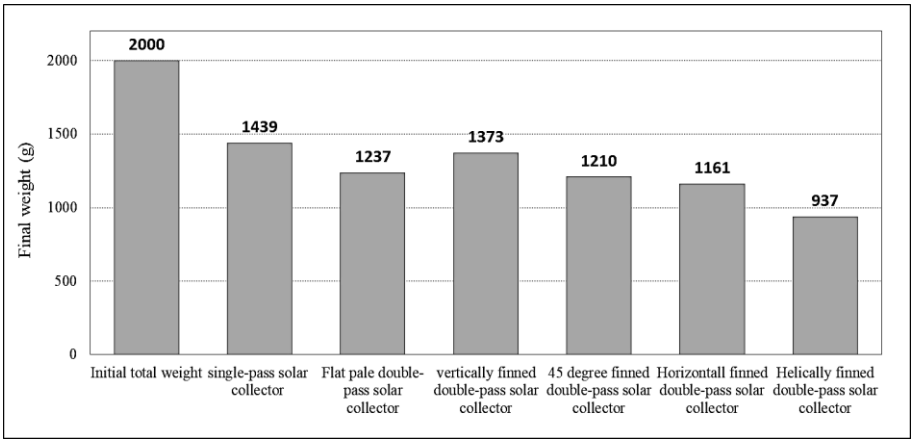


Fig. 23. The final total weight of dried product by using different solar air collectors

## 4. NEW SCIENTIFIC RESULTS

In this section the unique scientific results investigated in my study are shown as following:

*1. Air passes number of solar air collector*

Based on experimental results, I enhanced the instantaneous thermal efficiency of solar air collector by increasing the number of air passes from one to two passes. For justification of enhancement I developed a linear mathematical model can be applied for single and double passes types of solar collectors as:

$$\eta = a \frac{T_{av,s} - T_a}{I} + b.$$

I have identified the parameters of the model, *a* and *b*, for the ranges of experimental cases for single and double-pass solar collectors groups as following:

$a = -3308.3$ *and* $b = 168.8$ for single-pass solar collector group,

$a = -1881.8$ *and* $b = 63.09$ for double-pass solar collector group.

During the approximation the correlation coefficients were 0.42 and 0.335 along with the standard deviations of 7.76% and 3.62% for single and double-pass solar collectors, respectively. The models represent the closest expression of the relationship between temperature difference, solar radiation intensity and thermal instantaneous efficiency.

Consequently, I proved the improvement of the amount of evaporated moisture by using double-pass solar collector from dried product items (apple slices), and also that the temperature of air and relative humidity stratification curves of drying chamber trays are much influenced by useful heat and absorbing temperature curves.

*2. Direction and shape of extended surfaces*

I improved the experimental thermal efficiency of solar collector by using different shapes and directions of attached fins. Accordingly, I justified that the thermal efficiency of these types of solar collectors is related to the angle of attached fins introducing the following second order polynomial model:

$$\eta = a\,\psi^2 + b\,\psi + c.$$

I have identified the *a*, *b* and *c* parameters of rectangular finned double-pass solar air collectors groups as a=-0.0006, b=-0.0536 and c=55.975, respectively. During the approximation the correlation coefficient was 0.99 along with the standard deviation of 3.9%.

Based on the experimental and modelling results, I proved that the horizontal direction of rectangular extended surfaces (fins) attachment is the most efficient direction to get the maximum percentage of useful gained heat. I have pointed out that the vertical rectangular fins did not increased the thermal efficiency of solar collector significantly.

I have justified that the lost water content from dried product items by the horizontally finned solar collector was higher than the case of using flat, vertically finned or $45^o$ inclined finned plate solar air collector, as well the single-pass solar collector.

In other hand, I proved that a solar air collector with aluminium helical fins attachment has a significant thermal improvement in its instantaneous thermal efficiency and drying process time.

*3. Solar air collector overall daily performance*

I introduced the daily efficiency to evaluate the thermal performance of solar air collectors. Based on integrated daily experimental results I justified the overall enhancement of the solar collector's thermal behaviour by 7.3% caused by applying air passes duplication. Additionally, I have determined also the enhancements caused by changing the directions of extended surfaces (fins) which attached to the absorber surface, as follows: 11% for horizontal, 7% for 45 degree and 1% for vertical fins

I proved that the helically finned plate double air pass solar collector achieved the highest thermal daily efficiency (63.3%) compared to the other tested solar air collectors. The enhancement of thermal efficiency compared with flat plate solar collector (reference collector) was about 18%.

*4. Forced and natural air mass flow rate*

In case forced air movement, I proved that the thermal daily efficiency of solar air collector varies indirectly with variation of air mass flow rate of inline blower. The thermal performance of solar air collector investigated under four values of air mass flow rate, then I justified that the highest value of thermal efficiency was at highest air mass flow rate.

In case of natural air movement, I justified the increase of air speed with using circular shape of solar chimney. For that purpose, I have developed a second order polynomial model in order to determine the relation between the speed of air stream in circular chimneys versus solar radiation intensity in the operational range of 600 W/m$^2$ and 1100 W/m$^2$:

$$V_{ch} = 10^{-6}\, I^2 - 0.002\, I + 1.3806.$$

During the approximation the correlation coefficient was 0.96 along with the standard deviation of 0.075 m/s.

Additionally, I developed a linear model to estimate the speed of air in circular of chimneys in term of average temperature of absorbing surface for absorber temperature range between 70 and 83 $^o$C as following:

$$V_{ch} = 0.016\, T_{s,av} - 0.4709.$$

During the approximation the correlation coefficient was 0.57 along with the standard deviation of 0.082 m/s. I proved that the increasing of absorbing surface temperature leads to rise the temperature of air which resulted increasing of bouncy force. The little slope which done in the top of drying chamber leads to smooth movement of air flow.

*5. Final weight of dried product*

I evaluated and justified the enhancement of drying process in term of final weight by increasing number of air passes and using different shapes and directions of fins. I proved that using attached helical fins to absorber surface of double-pass solar air collector provides the lowest final weight of dried product items. After 5 hour drying period the product lost about 53% of its initial weight.

The changing of fins direction affected on the final weight of the dried product. I elaborated that in case of using the double-pass solar air collector the weight loss of material to be dried enhanced from 28% to 38% compared with single-pass solar air collector after 5 hour drying period. Attaching horizontal fins to the double-pass solar collector enhanced weight loss from 38% to 42% compared with flat plate double-pass solar collector for the same drying period.

# 5. CONCLUSIONS AND SUGGESTIONS

In conclusion, an experimental study has been carried out to investigate the performance of various types of solar air collectors for drying processes objectives. In this study, the effect of air pass number have been studied by a ccomparison between single-pass solar air collector and double-pass solar air collector. The results showed the single and double-pass solar air collector inlet, outlet and second pass temperatures are directly proportioning with the solar radiation intensity and ambient temperature. The high absorbing surface temperates lead to increasing of solar collector heat losses and useful heat gained at the same time. Additionally, the useful heat gained by using double-pass solar air collector much higher than the gained useful heat by using single-pass solar air collector which leads to higher thermal efficiency and drying rates.

The direction and shape of extended surfaces (fins) are played a significant factor to improve the thermal performance of solar air collectors and drying process. The horizontal direction of rectangular extended surfaces (fins) attachment is the most efficient direction to get the maximum percentage of useful gained. The vertical rectangular fins did not increase the thermal efficiency of solar collector significantly. The vertical direction of extended surfaces does not produce high air turbulence as noticed with horizontal fins or $45^{o}$ inclined fins which leads to highest air temperatures. The lost water content from dried product items by the horizontally finned solar collector was more than the evaporated water by using flat, vertically finned or $45^{o}$ inclined finned plate solar air collector, as well the single-pass solar collector. In case of attaching the aluminium helical fins, it has a significant thermal improvement of solar air collector by about 18% of daily thermal efficiency and gained useful heat. The drying process enhanced by using the helically-finned solar air collector. The evaporated water from the dried product (apple slices) was much higher than the collected experimental measurements by using the other types of tested solar air collectors. The helically-finned solar collector showed a significant enhancement of drying process due to increasing the evaporated water from the dried product with initial weight 2000 g.

The air temperature stratification curves of drying chamber five trays are much affected by useful heat and absorbing temperature curves. Also, the relative humidity stratification of air in the drying chamber trays are high at the beginning of experiments due to the high moisture content of dried product items, then decrease exponentially with the time of experiments and ambient relative humidity.

The effect of air mass flow rate had been invisigted. In case of forced air circulation, the thermal efficiency of solar collector proportions indirectly with the mass flow rate of air. The efficiency of double-pass solar collector increased signifigntly by increasing the flow rate of air. In case of natural air circulation, the speed of air is much affected by solar radiation and absorbing surface temperature by circular chimney integration.

For the future works, many ideas can be suggested to improve this work. The tested solar air collectors and dryer can be simulated by using one of the standard simulation software like Matlab or ANSYS. The changing of the shape of absorbing surface from rectangular to other shapes can improve the thermal efficiency of solar air collector such as twisted, perios fins, holed, circular fins, etc. The investigation of the performance of the tested solar collectors for other products drying can be suggested for the future projects. Additionally, the investigation of the thermal efficiency of the double-pass solar collector by the holed absorbing surface. The studied drying system can be developed to be controlled temperature and humidity.

# 6. SUMMARY

## PERFORMANCE ENHANCEMENT OF SOLAR AIR COLLECTORS APPLIED FOR DRYING PROCESSES

In this work, a comprehensive experimental investigation carried out to evaluate the thermal enhancement of solar air collector performance for drying purposes. The tested system consists of many essential parts: solar air collector, drying chamber, blower, and chimney. To achieve the aims of this research a six solar collectors are tested experimentally in the laboratory of Szent István University in Hungary. The first collector is a flat plate single-pass solar air collector while the second is a flat plate double-pass solar air collector. The third, fourth and fifth collector are horizontal, 45 degrees and vertically finned plate double-pass solar air collector respectively. The sixth collector is helically-finned plate double-pass solar air collector. The external dimensions of every collector are 50× 120×15 cm width, length, and depth respectively. The drying chamber has been made from 5 cm thick of polystyrene with 50×50×100 cm length, width, and height respectively. The chamber carried five trays where the dried product (apple slices) items must be put. To show the effect of forced and natural air mass flow rate, an inline air blower and 1.5 m circular section chimney are integrated with the solar system. The inline blower connected to PV module by a power supply regulator. The system is tested on many days and under different conditions of weather and air mass flow rates. The collected data such as humidity, temperature, radiation and flow speed are measured by using a calibrated instruments.

The results showed good agreements with previous studies. The results obtained that the useful heat gained by using double-pass solar air collector much higher than the gained useful heat by using single-pass solar air collector. The double-action of air pass number increased the daily thermal efficiency of solar air collector from 38.25% to 45.56%. The experimental results proved that the horizontal direction of attached fins is more efficient than the vertical and 45-degree direction. The experiments showed that the daily thermal efficiencies of flat, vertically finned, horizontally finned, 45 degrees finned, and helically-finned plate double-pass solar air collector are 45.56%, 46.53%, 56.01%, 52.84% and 63.3% respectively. The thermal efficiency of solar collector proportions indirectly with the mass flow rate of air. The efficiency of double-pass solar collector increased from 45.5% to 59% by increasing the flow rate from 0.0175 kg/s to 0.0251 kg/s. The speed of air is much affected by solar radiation and absorbing surface temperature by circular chimney integration.

The air temperature stratification curves of drying chamber five trays are much influenced by useful heat and absorbing temperature curves. Air relative humidity stratification of drying chamber trays are high at the beginning of experiments due to the high moisture content of dried product items, then decrease exponentially with the time of experiments and ambient relative humidity. The shape and size of dried apple slices are much changed after drying process. The color of slices became darker than the fresh slices due to the missed moisture content of product items.

The helically-finned solar collector showed a significant enhancement of drying process due to increasing the evaporated water from the dried product with original weight 2000 g. The final total weight of product items by using helically-finned collector was much less that final rcorded weights of propuct by using single-pass, flat plate double-pass, vertically finned, 45 degrees finned and horizontally finned plate solar air collector respectively.

## 7. THE MOST IMPORTANT PUBLICATIONS RELATED TO THE THESIS

*Refereed papers in foreign languages:*

1. **Al-Neama, M.A.,** Farkas, I. (2016): Influencing of solar drying performance by chimney effect, Hungarian Agricultural Engineering, Gödöllő, Hungary, Vol. 30, pp. 11-16. HU ISSN 0864-7410
2. **Al-Neama, M.A.,** Farkas, I. (2017): Investigation of finned solar air collector performance for drying purposes, R&D in Mechanical Engineering Letters, Gödöllő, Hungary, 2017, Vol. 16, pp. 64-72. HU ISSN 2060-3789
3. **Al-Neama, M.A.,** Farkas, I. (2018): Utilization of solar air collectors for product's drying processes, Journal of Scientific and Engineering Research, Vol. 5., No 2., 2018, pp. 40-56, ISSN 2394-2630
4. **Al-Neama, M.A.**, Farkas, I. (2018): Thermal efficiency of vertical and horizontal-finned solar collector integrated with forced air circulation dryer for apple as a sample, Drying Technology Journal, online version, ID: 1488260, DOI:10.1080/07373937.2018.1488260 (IF=2.219*)
5. **Al-Neama, M.A.,** Farkas, I. (2018): Evaluation of temperature and relative humidity stratifications in a solar drying chamber, Journal of Scientific and Engineering Research, ID: JSAER2018574. ISSN 2394-2630. (Accepted)

*International conference proceedings:*

6. **Al-Neama, M.A.,** Farkas, I. (2015): Study of solar energy drying system performance, Proceedings of the 5$^{th}$ European Drying Conference (EuroDrying'2015), Budapest, Hungary, October 21-23, 2015, pp. 22-27. ISBN 978-963-9970-62-5
7. **Al-Neama, M.A.**, Farkas, I.: Modeling of solar drying system with natural convection air flow, Proceedings of IDS 2016, 20$^{th}$ Internatinal Drying Symposium, Gifu, Japan, August 7-10, 2016, Paper No D-4-4, pp. 1-5.
8. **Al-Neama, M.A.,** Farkas, I. (2016): Modelling of a modular indirect natural convection solar dryer, Proceedings of EuroSun 2016 Conference, Palma, Spain, October 11-14, 2016, pp. 660-669, ISBN 978-3-9814659-6-9
9. **Al-Neama, M.A.,** Farkas, I. (2016): Energy analysis of active solar drying system connected with photovoltaic modules, Energy and the Environment, Croatian Solar Energy Association, Opatija, Croatia, October 26-28, 2016. pp. 187-196. ISBN 978-953-6886-23-4
10. **Al-Neama, M.A.,** Farkas, I. (2018): Flat plate solar air heater with helical integrated fins for drying processes, Proceedings of IDS 2018, 21$^{st}$ Internatinal Drying Symposium, Valencia, Spain, September 11-14, 2018, pp. 489-496. ISBN 978-84-9048-688-7

*Book chapter in foreign languages:*

11. **Al-Neama, M.A.**, Farkas, I. (2017): Design aspects of flat plate solar collectors used for drying applications, Towards sustainable agricultural and biosystems engineering, /ed. by A. Nyéki, A.J., Kovács, G. Milics/, Universitas-Győr Nonprofit Ltd, 2017, pp. 391-407, ISBN 978-615-5776-03-8